Published in Indian Journal of Pure and Applied Physics,

August (2006), Accepted Postprint

On the phase formation mechanism of $BaTiO_3$-$SrTiO_3$ solid solution through solid – oxide reaction

S.K.Rout [*], S.Panigrahi,

Department of Physics,

National Institute of Technology, Rourkela-769 008, India

Abstract

The formation of solid solution composition $Ba_{0.5}Sr_{0.5}TiO_3$, from $BaCO_3$, $SrCO_3$ and TiO_2 powders has been studied through solid oxide reactions using TGA/DSC, XRD. $BaCO_3$ decomposes at much lower temperature in the mixture due to the presence of acidic TiO_2. $BaTiO_3$ (BT) and $SrTiO_3$ (ST) start forming from the temperature $700^{O}C$ and $800^{O}C$ respectively without formation of BaO/SrO or any titanate phases. Rietveld refinement shows the rate of formation of BT is relatively higher than that of ST. The solid solution $Ba_{0.5}Sr_{0.5}TiO_3$ (BST (ss)) starts forming from $1000^{O}C$. The rate of formation of $BaTiO_3$ is higher than that of $SrTiO_3$. Activation energy for formation of $BaTiO_3$ (40.41 kcal/mol) is higher than that of $SrTiO_3$ (58.867 kcal/mol) in the system. Lattice parameter of initial solid solution phase is higher indicating that

[*] Author for correspondence. Tel.: +91-94370 85441
E- mail address: skrout@nitrkl.ac.in

the BST forms with the interface of BT. The final BST (ss) formation requires more activation energy (76.999 kcal/mol) than initial BT and ST.

Keywords: Perovskite; Phase formation kinetics; $BaTiO_3$-$SrTiO_3$; Solid solution

---

1. Introduction

A nonlinear ferroelectric with high dielectric constant materials $Ba_{1-x}Sr_xTiO_3$ (BST) have been widely investigated for their application as integrated storage capacitors in giga bit dynamic random access memory (DRAM). This is mainly due to their low dielectric loss, low leakage current, low temperature coefficient of dielectric constant and the composition dependent Curie temperature. In the DRAM operating temperature BST should be in paraelectric form to avoid fatigue and aging due to the ferroelectric domain switching[1-3]. In addition to the DRAM applications, BST have variety of other applications which are currently being studied such as hydrogen gas sensors[4,5], pyroelectric sensors[6,7] as a dielectric layer in electroluminescent display devices [8-10] and the new class of frequency tunable microwave devices, which include phase shifters, tunable filters, steerable antennas, varacters, frequency triplers, capacitors, oscillators, delay lines and parametric amplifiers etc.[11-14]. Each application listed above has its own material property requirement. Amazingly, BST materials fit into all these variety of applications because of their composition dependent properties. Simply by changing Ba/Sr ratio and also by adding aliovalent dopants the properties can be modified to fit into a given application. Rietveld's x-ray powder structure refinement based on simultaneous structure and microstructure refinement has been adopted in the present study because no other methods of

microstructure characterization are capable of determining the crystallite size, change in lattice parameters and relative phase abundances of all the phases in multiphase materials containing a large no of overlapping reflections. In the present study we investigated the phase formation and reaction mechanism of $Ba_{0.5}Sr_{0.5}TiO_3$ powder obtained by solid state reaction method using metal oxide precursors.

2. Experimental procedure

BST-solid solution was prepared by solid-state reaction route from $BaCO_3$ (S.D. Fine Chem., Mumbai), $SrCO_3$ (S.D. Fine Chem., Mumbai), and TiO_2 (E. Merck India Ltd.). All the powders were having more than 99% purity. Particle size of starting raw materials, measured using Malvern Mastersizer, are: $BaCO_3$ [D(v,0.1)=0.25 μm, D(v,0.5)=2.09 μm, D(v,0.9)=13.20 μm], $SrCO_3$ [D(v,0.1)=0.48μm, D(v,0.5)=13.13μm, D(v,0.9)= 14.63μm] and TiO_2 [D(v,0.1)=0.27 μm, D(v,0.5)=0.35 μm, D(v,0.9)=0.48 μm].The powders were thoroughly mixed in agate mortar using GR grade Isopropyl Alcohol (IPA) (E. Merck India Ltd.). Decomposition behavior of raw mixture, $SrCO_3$ and $BaCO_3$ were investigated using NETZSCH Thermal Analyzer. Mixed powder was calcined at various temperatures in the range 700^{o}C to 1500^{o}C for 1 hour to study the phase formation behavior. The calcined powders were characterized with respect to phase identification, phase quantity measurement, crystallite size determination and lattice parameter measurement etc., all by using Cu-K_α XRD (Xpert MPD, Philips, UK). For quantitative estimation of phases, calcined powders were analyzed using XRD at a step size of 0.02^o, 2θ with 10 second/step. The relative weight fractions were quantified using Rietveld refinement program MAUD[15]. Rietveld software MAUD is specially designed to refine simultaneously both the structural

and microstructural parameters along with the texture and residual stresses through a least square method. The peak shape was assumed to be a pseude-Voigt (pV) function with asymmetry. The background of each pattern was fitted by a polynomial function of degree four. The Rietveld method was successfully applied for determination of the quantitative phase abundances of the composite materials containing several crystallographic phase along with crystallite sizes of the different phases [16-18]. There is a simple relationship between the individual scale factor determined, considering all refined structural parameters of individual phases of a multiphase sample, and the phase concentration (volume/weight fraction) in the mixture. The weight fraction *(W_i)* for each phase was obtained from the refinement relation

$$w_i = \frac{S_j (ZMV)_i}{\sum_j S_j (ZMV)_j}$$

where *i* is the value of *j* for a particular phase among the *N* phases present, *Sj* the refined scale factor, *Z* the number of formula units per cell, *M* the atomic weight of the formula unit and *V* the volume of the unit cell. The structure refinement along with size–strain broadening analysis was carried out simultaneously by adopting the standard procedure [15,19,20].

3. Results and Discussion

Fig.1 shows DSC-TG tracing of raw mixture. TG graph shows a continuous wt loss from about 700 ^{O}C to 1275 ^{O}C. The DSC graph shows four endothermic peak at 728 ^{O}C, 806.7 ^{O}C, 928^{o}C and 1156 ^{o}C. The small peak at 728 ^{O}C corresponding to ~0.8 % wt loss of the precursor. This weight loss may be attributed to the decomposition of very fine $BaCO_3$ particles present in the precursor. As previously reported by

author, $BaCO_3$ raw material has finer particle fraction D(v,0.1)=0.25 μm and these fractions decomposes at lower temperature in presence of TiO_2 [21]. As no weight loss found under the peak at 806.7 for $BaCO_3$ decomposition it is corresponds to polymorphic transformations of rhombohedral to hexagonal (gamma -- Beta) structure (this peaks theoretically occurs at 806 C) [22]. The hexagonal to cubic (beta - -alpha) transformation peak which occurs at 986 C [23] is not observed in the precursor. Both the peaks were prominent in case of pure $BaCO_3$. The endothermic peak at 928^oC due to the polymorphic transformation of $SrCO_3$ from the orthorhombic space group (Pmcn) to the rhombohedral space group (R-3m)[24]. The huge 1156^oC endothermic peak corresponds to the major decomposition of both $BaCO_3$ and $SrCO_3$ in the precursor. However, in pure $BaCO_3$ that peak occurs at about 1130^0C and in pure $SrCO_3$ that peak occurs at about 1187^oC. This overlapping decomposing peak occurs in between the decomposition temperature of $BaCO_3$ and $SrCO_3$ in the precursor may be due to the large difference between their particle sizes and due to the presence of acidic TiO_2 in the mixture[25].

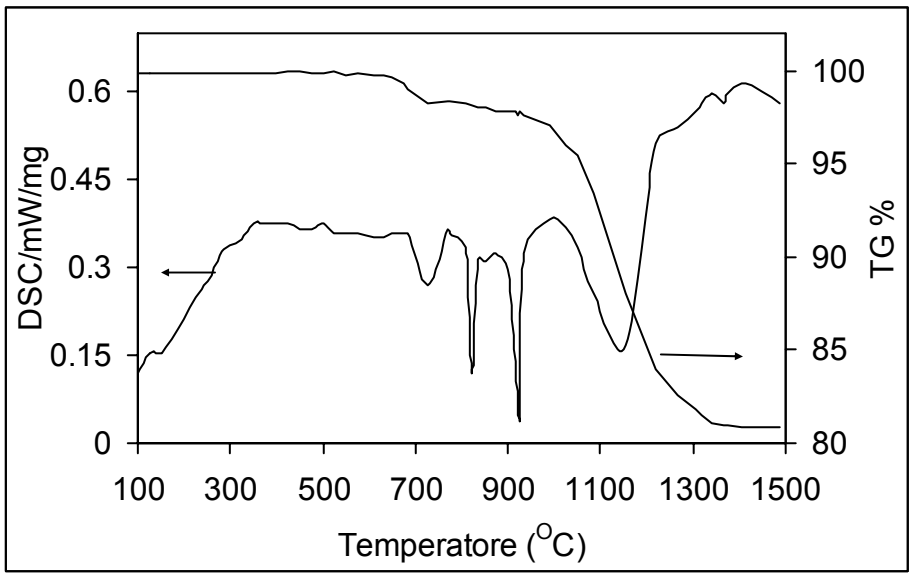

Fig.1. TGA and DSC curve in air for the $BaCO_3$, $SrCO_3$ and TiO_2 powder mixture.

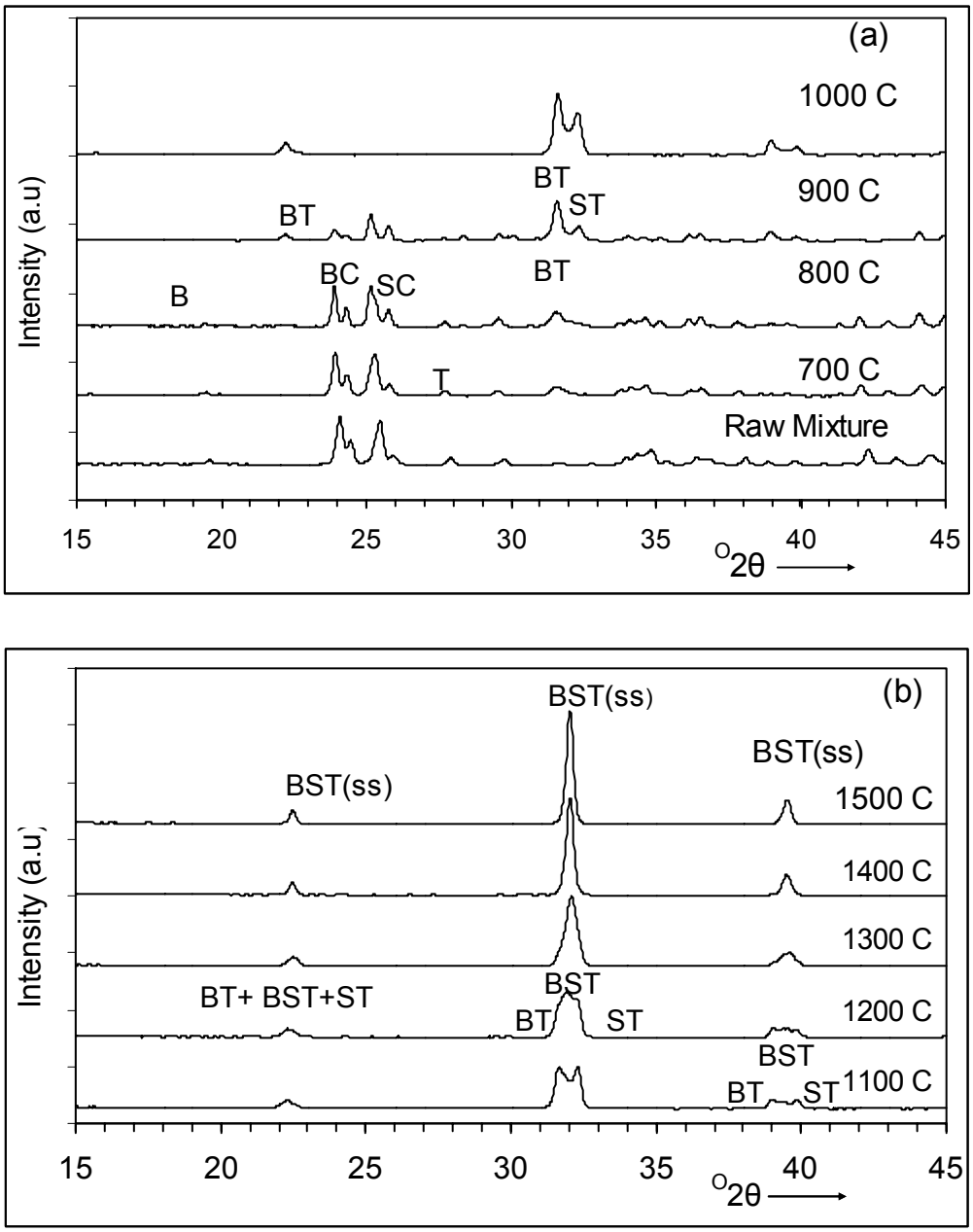

Fig. 2. Room temperature XRD patterns of raw mixture and calcined precursor powder for 1 h (a) Raw mixture, 700,800,900 and 1000 ^{O}C; (b) at 1100,

1200,1300,1400 and 1500 ^{O}C; with notations BC=$BaCO_3$, SC= $SrCO_3$,BT=$BaTiO_3$, ST=$SrTiO_3$, BST(ss)=$Ba_{0.5}Sr_{0.5}TiO_3$.

Fig. 2 shows XRD pattern of raw precursor powder and powder calcined at different temperature for 1 hour. It shows that BT and ST forms in the system coherently with BST formation. Slow step scanning XRD analysis reveals that BT starts forming from 700 ^{O}C and ST starts forming from 800 ^{O}C. Formation of BaO or other phases like Ba_2TiO_4 or $BaTi_3O_7$, has not been observed within the detection limit of XRD. These phases were not also observed with the presence of both Ti and Zr[21]. Here BT is directly formed through the reaction $BaCO_3$ +TiO_2=$BaTiO_3$+CO_2(g).The intermediate phases like Sr_2TiO_4 and $SrTi_3O_7$ were observed in the samples calcined at 1000 ^{O}C for 1h and at 1100 ^{O}C for 1h, with the presence of both Ti and Zr[25]. But in the present case these phases were not observed may be due to the presence of more acidic TiO_2 than ZrO_2 in the system and ST is directly formed through the reaction $SrCO_3$ +TiO_2=$SrTiO_3$+CO_2(g).

The XRD patterns also suggest that the rate of formation of $SrTiO_3$ is lower than the formation of $BaTio_3$, which may be due to the (i) presence of more stable Sr than Ba [26,27] in the system and/or (ii) high average particle size of $SrCO_3$ than $BaCO_3$. BST(ss) starts forming from 900^{O}C coherently with both BT and ST. Variation of their phase content with calcinations temperature is shown in the fig.3. Rietveld refinement shows maximum volume of BT and ST phases in samples of 1000^{O}C/1hour and 1100^{O}C/1hour respectively. These quantities at that temperature were considered 100%.

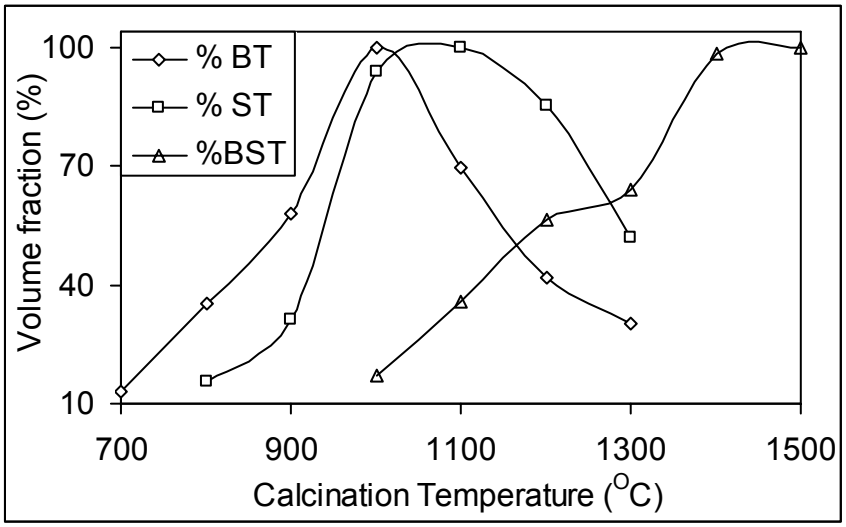

Fig. 3. Non-isothermal transformation kinetics of precursor in static air.

The quantity of BT is always higher than ST at ant temperature up to 1000 ^{O}C; but after 1000 ^{O}C, the quantity of BT decreases quickly than ST and the quantity of BST (ss) increases rapidly. These observations indicate that $BaTiO_3$ forms easily in the system through solid-state reaction between $BaCO_3$ and TiO_2 and the rate of ST formation is relatively slower. However, quantity of BT increases slowly near the temperature 900^{o}C, which may be due to the decrease in the finer fraction of $BaCO_3$ and TiO_2 reactants, as they are used to form BT in the lower temperature range. Above 1300^{o}C, BST (ss) increases rapidly due to inter-diffusion between BT and ST.

Figure 4 represents the final output after structural refinements for the $Ba_{0.5}Sr_{0.5}TiO_3$ phase using Rietveld structural refinement program. Structural refinements were carried out, initially taking the end member reference for the cubic (space group Pm3m) compound $SrTiO_3$. The initial lattice structural parameter was calculated from the reflections and correcting with CCP14 program “Checkcell”. The Wyckoff positions were taken from the Wyckoff’s series. The structural refinement showed that the composition $Ba_{0.5}Sr_{0.5}TiO_3$ is cubic with space group Pm3m. The

occupancy factors for the mixed Ba and Sr sites were fixed at the nominal composition. The Ba and Sr displacement parameters were constrained to be equal. Refined parameters included scale factor, background coefficient, profile coefficients, and anisotropic thermal displacement parameters. During the refinement fitting of both background and diffraction intensities were taken care by interactive method. The refinements produced satisfactory agreement factors R_{wp} (weighted residual error), R_p (Brag factor) and R_{exp} (expected error) for 5500 observations and 42 variables (fig.4) and given in the captions of the figure 4. Goodness of fit was calculated from refinement agreement factors: ($GoF=R_{wp}/R_{exp}$).Refinement continues till convergence is reached with the value of the quality factor, GoF approaching 1. In the present composition the GoF is found to be 1.23, which confirms the goodness of the refinement within the permissible range of error.

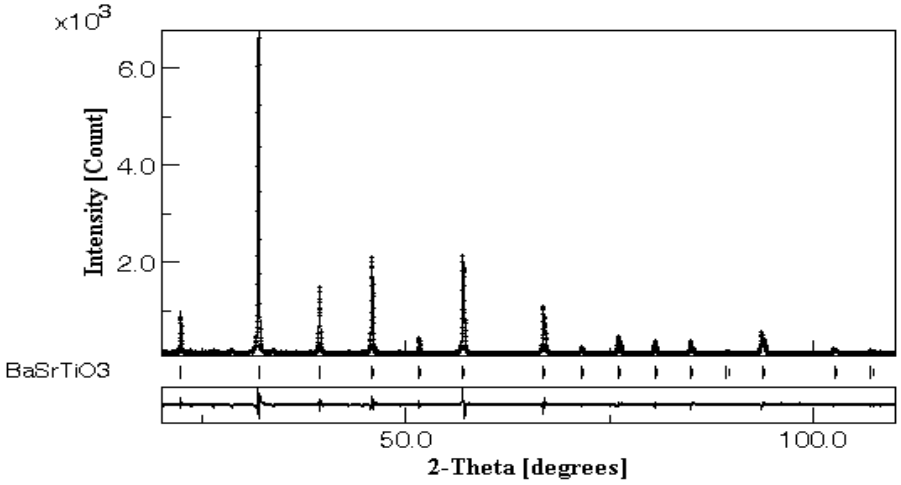

Fig.4. Observed (▪), calculated (—) and residual (lower) X -ray powder diffraction patterns of $Ba_{0.5}Sr_{0.5}TiO_3$ composition revealed from Rietveld's powder structure refinement analysis. Peak positions of the phases are shown at the base line as

small markers (l). R_{wp} (%) = 8.56074, R_p (%) = 6.92393,R_{exp} (%) = 6.670418, and Sigma= 1.2364

The atom positional parameters for the composition $Ba_{0.5}Sr_{0.5}TiO_3$ are: Ba/Sr 1a (0,0,0), Ti 1b (1/2,1/2,1/2) and O 3c (0,1/2,1/2). The isotropic thermal (displacement) parameters (β_{iso} x 100Å^2) are: Ba/Sr (1.618), Ti (1.183) and O(0.7167). The symmetry constraints on the thermal parameters in the *Pm3m* space group are as following: for Ba, Ti and Zr $U_{11}=U_{22}=U_{33}$, $U_{12}=U_{13}=U_{23}=0$, for O $U_{22}=U_{33}$, $U_{12}=U_{13}=U_{23}=0$. But these anisotropic displacements of the various atoms in powder diffraction experiments X-rays are somewhat insensitive to the exact direction of the anisotropic movements which could be best monitored in neutron diffraction or high energy synchrotron radiation.

To check the phase formation kinetics, concentrations of the phases were used to measure the activation energy for their formation using the following Avrami-Mehl diffusion based relationship [28]:

$$[1- [(1-X_B)^{1/3}]^2 = 2Kt/R^2$$

Where $2K/R^2$ is essentially a reaction rate constant, X_B is the volume fraction reacted at time 't'. Ln (K/R^2) vs. 1/T plot represents Arrhenius expression and ativation energy for the phase formation can be derived from the slope of the plot.

Fig.5 shows temperature dependency of formation reaction of different phases. They show Arrhenius type of linear temperature dependency. Activation energy measured from slop shows that BT formation requires less activation energy (40.41 kcal/mol) than that of ST formation (58.867 kcal/mol). Activation energy required for formation of BT and ST in the present system is higher than that reported else where [21,25]. Here higher activation energy required may be due to simultaneous formation of BT, ST in the temperature range 800^{O}C to 1000^{O}C and

BT, ST with BST(ss) at the temperature 1000^{O}C. Phases were formed in this system through solid state interdiffusion between different particles. Interdiffusion takes place with different ions limiting the speed of diffusion. Activation energy results shows that phase formation reaction may be limited by the diffusion of Ba for BT and Sr for ST formation respectively. In this case Ti and O are assumed to be immobile because their concentrations are spatially invariant. Since Sr ion is more stable, it's diffusion requires more activation energy to form perovskite phase. BST solid solution formation requires less activation energy (43.41 kcal/mol) in the temperature range 900^{O}C to 1200^{O}C but requires relatively high activation energy (76.999 kcal/mol) in the temperature range 1300^{O}C to 1500^{0}O. The activation energy in the temperature range 1200^{O}C to 1300^{O}C is not calculated due to temporary slow down in the formation kinetics. The activation energy for formation of BST (ss) in the lower temperature range is close to the activation energy of BT formation. This observation indicated that the formation of the BST (ss) in the lower temperature range is more coherent to BT not to ST. i.e the BST (ss) forms in the BT site rather than ST site. The study also indicates that solid solution formation takes place by the diffusion of BT into ST lattice, as BT decays more rapidly than ST at higher temperature. Also from XRD data it also indicated that solid -solution formation takes place by the interdiffusion of BT into ST lattice. As the peaks of ST are sifting towards lower angle with increase in calcinations temperature from 800^{O}C to 1000^{O}C, indicating increase in unit cell Volume (Table 1) due to the incorporation of bigger Ba $^{2+}$ ions. Where as, lattice parameter of BT remains constant in the said temperature range (Table 1) indicating no diffusion of Sr $^{2+}$ in to BT lattice. At the temperatures 1100^{O}C and above the peaks of BT shifts towards higher angle and lattice parameter of BT

decreases (Table 1), where as the lattice parameter of ST remains increasing, indicating the incorporation of Sr^{2+} into Ba^{2+} ions and vice versa.

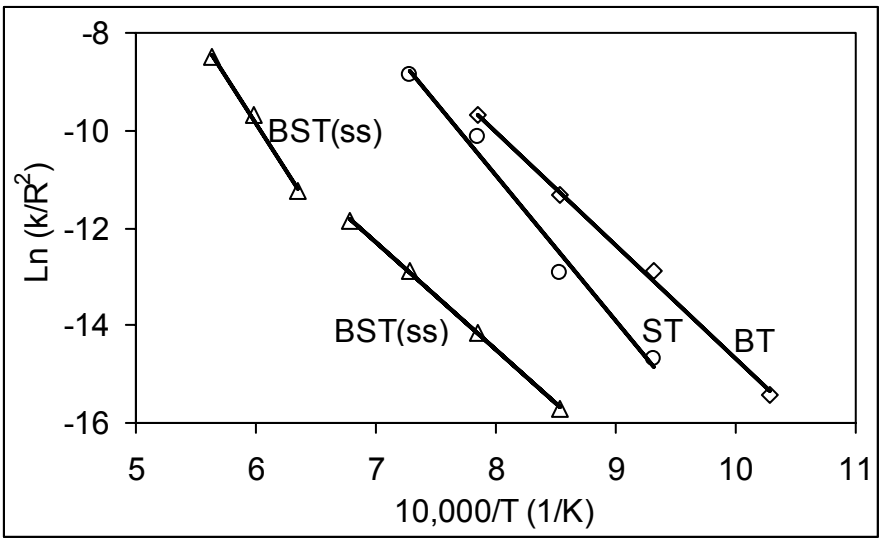

Fig. 5. Arrhenius dependence of reaction rate on calcination temperature for the transformation of precursor to $BaTiO_3$ (◊) and $SrTiO_3$ (o) and then to $Ba_{0.5}Sr_{0.5}TiO_3$ solid solution (Δ).

The room temperature lattice parameters of three different phases at different temperatures along with their x-ray crystallite size are shown in table 1. Lattice parameter of phases were calculated considering the cubic structure for BT (as per JCPDs card No 79-2263), structure for ST (as per JCPDs card No.84-0444 and also the cubic structure for BST (as per JCPDs card No.39-1395.). Lattice parameter of BST (ss), found in the present study (a_0= 3.952Å) is similar to that reported (a_0= 3.947 Å) in JCPDs card No.39-1395). Previously we have indicated that initially the solid-solution formation takes place by the diffusion of BT in to ST lattice and at higher temperature both the diffusion (i.e ST into BT and BT in to ST) takes place. The XRD peaks of BST (ss) which forms in between [110] peak of BT and [110] peak of ST (Fig.2 b) was indexed as [110] reflections of cubic BST (ss) phase. That

indicates that the solid solution is formed coherently with [110] peak of BT at lower temperature and with [110] peak of ST at higher temperature. A similar coherent interface between $BaZrO_3$ and $Ba(Ti_{0.6}Zr_{0.4})O_3$ lattices and $SrZrO_3$ with $Sr(Ti_{0.5}Zr_{0.5})O_3$ were also reported by the authors [21]. This mechanism also suggests that the morphology of BST (ss) should be controlled by the morphology of ST and BT phase formed in the intermediate stage. Table 1 also shows the XRD crystallite sizes of BT, ST and BST (ss) at different temperatures. Crystallite size of BT is relatively higher than ST, which again indicates the easy formation of BT in the system.

Table 1

Lattice parameter 'a_0' in Å and XRD-crystallite size in nm of BT, ST and BST (ss) in the samples calcined at different temperatures.

Calcination	$BaTiO_3$		$SrTiO_3$		BST (ss)	
Temp.(°C)	a_0 (Å)	Crystallite Size (nm)	a_0 (Å)	Crystallite Size (nm)	a_0 (Å)	Crystallite Size (nm)
700	4.0065(8)	44.171				
800	4.0065(8)	43.762	3.9150(4)	23.776		
900	4.0066(3)	43.132	3.9196(9)	35.608		
1000	4.0065(2)	42.146	3.9238(9)	40.824	3.9850(7)	24.7205
1100	3.9978(7)	48.659	3.9169(7)	50.464	3.9802(4)	25.2730
1200	3.9962(4)	50.045	3.9202(7)	47.123	3.9756(4)	26.7247
1300	3.9949(6)	30.245	3.9301(4)	50.259	3.9433(4)	33.1065
1400	--------	-------	--------	--------	3.9532(4)	40.3569
1500	--------	-------	--------	--------	3.9529(4)	49.0520

Note. The numbers in the parentheses are the estimated standard deviations.

4. Conclusions

The formation kinetics of $BaTiO_3$-$SrTiO_3$ solid solution from mixture of $BaCO_3$, $SrCO_3$ and TiO_2 powders has been studied in air at 700-1500^{O}C using TGA/DSC and XRD. Based on non isothermal kinetic analysis and on crystal structure, the reaction mechanism can be described by a two step process:

(1) During first step, $BaTiO_3$ and $SrTiO_3$ phases are formed through direct solid state reaction between $BaCO_3$, $SrCO_3$ and TiO_2 at lower temperature. The phases like Ba_2TiO_4, $BaTi_3O_7$, Sr_2TiO_4 or $SrTi_3O_7$ etc., has not been detected. $BaTiO_3$ formation requires less activation energy than $SrTiO_3$, which may be due to the difference in their ionic radius and stability of the Sr and Ba[22]. The BST(ss) forms coherently with BT at lower temperature.

(2) During the second step, at relatively higher temperature, BST solid solution is formed due to the diffusion of $BaTiO_3$ and $SrTiO_3$. Activation energy for this step is relatively higher.

References

1. Kawano H, Mori K & Nakayama Y, *J Appl Phys* **73** (1993) 5141.
2. Horikawa T, Makita T, Kuroiwa T & Mikami N, *Jpn J Appl Phys* **34** (1995) 5478.
3. Abe K, Yanase N, Komatsu S, Sano K, Fukushima N, & Kawakubo T, *IEICE Trans. Electron E* 81-C (1998) 505.
4. Zhu W, Tan O K & Yao X, *J Appl Phys* **84** (1998)5134.
5. Zhu W, Tan O K, Deng J & Oh JT, *J Mater Res* **15** (2000)1291.
6. Noda M, Hashimoto K, Kubo R, Tanaka H, Mukaigawa T, Xu H & Okuyama M *Sens Actua* **77** (1999) 39.

7. Cheng J G, Meng X J, Li B, Tang J, Guo S L, Chu J H, Wang M, Wang H & Wang Z, *Appl Phys Lett* **75** (1999)2132.
8. Zhang H X, Kam C H, Zhou Y, Han X Q, Lam Y L, Chan Y C & Pita K, *Materials Chem and Physics* **63** (2000)174.
9. Song M H, Lee Y H, Hahn T S, Oh M H & Yoon K H, *Solid State Electronics* **42** (1998) 1711.
10. Song M H, Lee Y H, Hahn TS, Oh M H & Yoon K H, *J Kor Ceram Soc* **32** (1995)761.
11. Sengupta L C & Sengupta S, *IEEE Trans on Ultrasonics, Ferroelectrics and Frequency Control* **44** (1997) 792.
12. Miranda F A, Romanofsky R, Van Keuls F W, Mueller C H, Treece R E & Rivkin T E, *Integr Ferroelectrics* **17** (1998) 231.
13. Chang W, Horwitz J S, Carter A C, Pond J M, Kirchoefer S W, Jlmore C M & Chrisey D B, *Appl Phys Lett* **72 (**1999)1033.
14. Zafar S, Jones R E, Chu P, White B, Jiang B, Taylor D, Zurcher P, Gillepsie S, *Appl Phys Lett* **72** (1998) 2820.
15. Lutterotti L, *Maud version 1.99*, 2004, http://www. Ing.unitn.it/maud.
16. Dutta H, Sahu P, Pradhan S K, & De M, *Mater Chem Phys* 77 (2002)153.
17. Lutterotti L, Scardi P & Maistrelli P, *J Appl Crystallogr* 25, 459 (1992)
18. Yang R A, & Wiles B D, *J Appl Cryst* 15, 430 (1982).
19. Pal H, Chanda A, De M, *J Alloys Compd* 278,209 (1998).
20. Warren B E, *X-ray diffraction, Addition-Wesley, Reading, MA, 1969, Chapter 13*.
21. Bera J, Rout S K, *Materials letter* **59 (**2005)135-138

22. Perry's Chemical Engineers' Handbook, 6th Edition, edited by Robert H. Perry, Don W. Green, and James O. Maloney (McGraw-Hill Book Company, New York, 1984), p. 3-8.
23. Evans R C. *An Introduction to Crystal Chemistry, Cambridge University Press, Cambridge, UK*, (1996), p.410
24. Stockenhuber M, Mayer H, & Lercher J A, *J Am Cerm Soc* **76**[5] (1993) 1185.
25. Bera J & Rout S K, *Materials Research Buletin* **40** (2005) 1187-1193.
26. Rase D E & Roy R, *J Am Ceram Soc* 38[3] (1955)111.
27. Drys Miroslawa, Trzebiatowski W, *Rodzniki Chem* 31 (1957) 492.
28. Terry A Ring, *Fundamentals of Ceramic Powder Processing and Synthesis, Academic Press, Inc. 1996, pp* 174.